of the effects of environment conditions on the performance of charring ablators," *AIAA Entry Technology Conference* (American Institute of Aeronautics and Astronautics, New York, 1964), pp. 259–269.

[73] Babish, C. A., III, "Hyperflo supersonic parachute," Air Force Flight Dynamics Lab., RTD Technology Briefs, Vol. I, no. 11 (November 1963).

[74] Turner, R. D., "A recovery system for a controlled descent through the martian atmosphere," Cook Electric Co.

[75] Daigle, D. L. and Lonborg, J. O., "Evaluation of certain crushable materials," Jet Propulsion Lab. TR 32-120 (January 13, 1961).

[76] McFarland, R. K., Jr., "Hexagonal cell structures under post-buckling axial load," AIAA J. 1, 1380–1385 (1963).

[77] Hanel, R. A., Richtmeyer, L. E., Stampfl, R. A., and Stroud, W. G., "Experiments from a small probe which enters the atmosphere of Mars," NASA TN D-1899 (December 1963).

[78] Vicente, F. A., "The effects of various reentry vehicle parameters on R-F attenuation," Aerospace Corp., BSD TDR-63-227 (October 28, 1963).

MARCH-APRIL 1965 J. SPACECRAFT VOL. 2, NO. 2

Similarity Criteria for Thermal Modeling of Spacecraft

B. T. Chao* and G. L. Wedekind†
University of Illinois, Urbana, Ill.

General scaling criteria for thermal modeling of spacecraft are deduced from governing equations of the temperature field for both two- and three-dimensional cases. Surfaces are assumed to be opaque and nondiffuse; variations of bulk thermal properties with temperature are considered. Two techniques, namely, temperature preservation and material preservation, are examined in detail. Difficulties of perfect modeling are pointed out and possible compromises are suggested. For two-dimensional problems, a significant advantage may be obtained by employing models of distorted thickness. Control of apparent thermal conductivity of materials by slitting offers interesting possibilities for both steady and nonsteady simulation.

Nomenclature

Any consistent system of units may be used; the engineering system is indicated below.

a = exponent in the power function describing the dependence of thermal conductivity on temperature
A = surface area, ft^2; A' = dimensionless area, A/L^2
b = exponent in the power function describing the dependence of heat capacity on temperature
c = heat capacity, Btu/ft^3-°R
d = thickness, ft
E_s = solar radiation, $\int_0^\infty E_{s,\lambda}d\lambda$, Btu/hr-ft^2; E_s' = dimensionless solar radiation
$E_{s,\lambda}$ = monochromatic solar radiation, Btu/hr-ft^2-μ
h_J = joint conductance, Btu/hr-ft^2-°R
I_λ = monochromatic intensity of radiosity, the rate at which radiant energy leaves a surface in the direction θ, ϕ, per unit solid angle, per unit wavelength, per unit surface area perpendicular to the pencil of rays, Btu/hr-ft^2-μ sr; thus, for surface element dA_i, it is understood that $I_{\lambda,i} = I_{\lambda,i}(T_i, \theta_i, \phi_i)$
I = intensity of radiosity, $\int_0^\infty I_\lambda d\lambda$, Btu/hr-ft^2-sr; hence I implies $I(T, \theta, \phi)$; I' = dimensionless intensity of radiosity, $I/\sigma T_0^4$
$I_{b,\lambda}$ = monochromatic intensity of radiation of a black surface, $(1/\pi)C_1\lambda^{-5}/\{[\exp(C_2/\lambda T)] - 1\}$, where $C_1 = 1.1870 \times 10^8$ Btu-μ^4/hr-ft^2, $C_2 = 2.5896 \times 10^4$ μ-°R
k = thermal conductivity, Btu/hr-ft-°R
L = characteristic length, ft
q_A = prescribed surface heat flux, Btu/hr-ft^2
q_{net} = net rate at which radiation leaves a surface, Btu/hr-ft^2; q_{net}' = dimensionless net rate at which radiation leaves a surface, $q_{net}/\sigma T_0^4$
r = distance between surface elements (see Fig. 1), ft
S = rate of internal heat generation per unit volume, Btu/hr-ft^3
t = time, hr; t' = dimensionless time (Fourier number), $\bar{k}T_0^a t/\bar{c}T_0^b L^2$
T = temperature, °R; T' = dimensionless temperature, T/T_0
T_0 = characteristic temperature of the problem, °R
x, y = curvilinear orthogonal coordinates (see Fig. 1), ft; x', y' = dimensionless curvilinear orthogonal coordinates, x/L, y/L
α, γ = angles defining the direction at which incoming radiation strikes a surface coming from another surface (see Fig. 1)
β, ψ = angles defining the direction at which incoming collimated solar radiation strikes a surface (see Fig. 1)
δ, ξ = angles defining the direction at which incoming radiation strikes a surface coming from another part of the same surface (see Fig. 1)
ϵ_λ = directional monochromatic emissivity, $\epsilon_\lambda(T, \theta, \phi)$
θ, ϕ = angles defining the direction at which radiation leaves a surface (see Fig. 1)
λ = wavelength, μ
$\pi^{-1}\rho_\lambda(\alpha, \gamma)$ = monochromatic reflection function, the ratio of the rate at which monochromatic radiation is reflected from a surface in the direction θ, ϕ per unit solid angle, per unit surface area perpendicular to the pencil of rays, to the rate at which monochromatic radiation strikes a surface coming from the direction α, γ; thus, for surface element dA_i, $\pi^{-1}\rho_{\lambda,i}(\alpha, \gamma)$ implies $\pi^{-1}\rho_{\lambda,i}(T_i, \theta_i, \phi_i; \alpha_i, \gamma_i)$, and $\pi^{-1}\rho_{\lambda,i}(\delta, \xi)$ implies $\pi^{-1}\rho_{\lambda,i}(T_i, \theta_i, \phi_i; \delta_i, \xi_i)$, etc.
σ = Stefan-Boltzmann constant, 1.713×10^{-9} Btu/hr-ft^2-°R^4
ω = solid angle, sr

Received May 7, 1964; revision received October 13, 1964. The authors wish to thank J. M. F. Vickers of the Jet Propulsion Laboratory, California Institute of Technology, for his helpful suggestions during the preparation of this manuscript.

* Professor of Mechanical Engineering and Nuclear Engineering.

† Assistant in Mechanical Engineering.

Table 1 Coefficients for thermal conductivity ($k = \bar{k}T^a$), heat capacity ($c = \bar{c}T^b$), and values of ($a - b$) for six materials

Code[a]	Material	a	$\bar{k}$	b	$\bar{c}$	$a - b$
301 SS	301 stainless steel	0.395	0.733	0.221	13.7	0.174
Mg	AN-M-29 magnesium	0.497	1.99	0.226	6.4	0.271
Al	2024-T4 aluminum	0.580	1.93	0.302	5.27	0.278
Monel	Monel "K"	0.555	0.315	0.210	13.7	0.345
Steel	SAE 1010 steel	−0.485	815	0.400	4.05	−0.885
Be	Beryllium (96.5% pure)	−0.656	6700	0.417	3.9	−1.073

[a] Code used in Fig. 2.

Superscript

* = quantities associated with the model

Subscripts

i, j = quantities associated with surface A_i and A_j, respectively

(i) = quantities associated with A_i, but excluding the differential element dA_i

Introduction

MUCH of the complex electronic equipment and instrumentation being used on spacecraft must be maintained within fairly narrow temperature limits if dependable operation is to be assured. The ability to design a spacecraft such that the temperatures of the various components are maintained within these prescribed limits becomes a major problem. The difficulties encountered in coping with absorption, emission, and reflection from nondiffuse, opaque surfaces are further aggravated by the geometric complexities of the spacecraft. An analytical solution to the actual problem is extremely difficult, if not completely impossible.

Recently, much effort has been directed toward experimental techniques in simulating a space environment.[1–4] A prototype of the spacecraft can be tested under simulated flight conditions and modifications made in order to keep the temperatures within the prescribed limits.[5, 6] Accurate simulation of a space environment becomes increasingly more difficult as the size of the spacecraft increases. Such difficulties provide the impetus for investigating the possibilities of testing scaled-down models and deducing therefrom the information necessary to predict, with reasonable accuracy, the thermal characteristics of the spacecraft during an actual flight.

There are two general approaches that may be taken in attempting to establish the conditions required for complete similarity between a model and its prototype.

Dimensional analysis, based upon physical intuition and strict algebraic formalism, may be used to ascertain the dimensionless groupings that are pertinent to the problem. The model and prototype are said to be similar when these dimensionless parameters have the same value for the model as for the prototype.[7] Katzoff[8] adopted this approach to the thermal modeling of spacecraft. Others simply presented a list of such groupings without giving formal derivation.[5, 9, 10] Although the algebraic approach has the important merit of being simple and extremely general, it often has the drawback of not yielding all of the parameters that fully and correctly describe the process under consideration. Since the physical processes involved in the title problem are reasonably well understood, a reliable and more informative approach is to start from the governing equations of the temperature field and the associated initial and boundary conditions. This procedure is followed in this paper. Such an approach has been used by Wainwright et al.[11] but their formulation is not as general as is possible.

In the following, a detailed analysis of problems involving two-dimensional temperature fields will first be presented. The prototype is conceived to be fabricated of plates or sheets of uniform thickness, but otherwise of arbitrary shape and orientation (Fig. 1). All surfaces are opaque but not necessarily diffuse. The only external irradiation is assumed to be collimated solar radiation. The temperature fields considered are, in general, nonsteady. The preceding has been selected for study since, as we shall see later, it offers better possibilities of satisfying the scaling criteria and is still useful for certain spacecraft applications. Results for the three-dimensional case will be given and discussed.

Analysis

The following assumptions are made:

1) Surfaces are located in a space environment–black surroundings at 0°R.‡ The only external irradiation on the surfaces is assumed to be collimated solar radiation (but the results are applicable when other external irradiation, such as from the earth, is present).

2) The sheets are fabricated from isotropic, homogeneous materials. Their thermal conductivities and heat capacities are temperature dependent and are expressible as power functions according to

$$k = \bar{k}T^a \qquad c = \bar{c}T^b \tag{1}$$

A survey of literature indicates that (1) can adequately represent these properties for many materials within wide temperature ranges.[12–14] The data for six representative metals are shown plotted in Fig. 2, and their coefficients are given in Table 1. The data for beryllium were obtained from Ref. 12, and the rest are from Ref. 13.

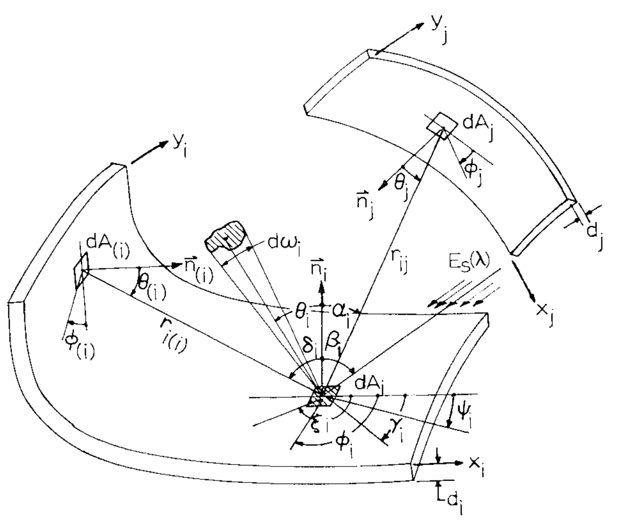

Fig. 1 Geometrical configurations considered in two-dimensional analysis.

‡ J. M. F. Vickers kindly pointed out that if the spacecraft were to operate between 429°R and 660°R (as is usually the case) the error involved in assuming 0°R and the use of liquid nitrogen cooled vacuum chamber in model testing is less than 1%.

3) The surfaces are opaque and are able to see themselves. Their surface properties are dependent upon temperature, direction, and wavelength of radiation.

Using the curvilinear coordinate systems illustrated in Fig. 1, the temperature fields are expressible as $T_i = T_i(x_i, y_i, t)$, with $i = 1, 2, \ldots, n$, n being the total number of surfaces involved. The governing nonlinear, integrodifferential equation for T_i is,

$$\frac{\partial}{\partial x_i}\left(k_i \frac{\partial T}{\partial x_i}\right) + \frac{\partial}{\partial y_i}\left(k_i \frac{\partial T}{\partial y_i}\right) - \frac{q_{\text{net},i}}{d_i} + S_i = c_i \frac{\partial T_i}{\partial t} \qquad (2)$$

where

$$q_{\text{net},i} = \int_{hs} I_i \cos\theta_i d\omega_i - \sum_{j \neq i} \int_{A_j} I_j \frac{\cos\alpha_i \cos\theta_j}{r_{ij}^2} dA_j - \int_{A(i)} I_{(i)} \frac{\cos\delta_i \cos\theta_{(i)}}{r_{i(i)}^2} dA_{(i)} - E_s \cos\beta_i \qquad (3)$$

In (3), the first term on the right-hand side represents the local radiosity, the abbreviation *hs* stands for the half-space on one side of the surface under consideration. The second term represents the local irradiation due to the radiant energy leaving all other surfaces in the configuration. The third term represents the local irradiation due to radiant energy leaving the rest of A_i and will clearly vanish if A_i is a convex or plane surface. The last term represents the local irradiation due to the collimated solar radiation.

The intensity of radiosity I for an opaque surface consists of radiation emitted and reflected by the surface. Hence,

$$I_i = \int_0^\infty I_{b,\lambda}(T_i)\epsilon_{\lambda,i}\, d\lambda + \sum_{j \neq i} \frac{\cos\alpha_i \cos\theta_j}{r_{ij}^2} \times dA_j \int_0^\infty I_{\lambda,j} \frac{1}{\pi} \rho_{\lambda,i}(\alpha, \gamma) d\lambda + \int_{A(i)} \frac{\cos\delta_i \cos\theta_{(i)}}{r_{i(i)}^2} \times dA_{(i)} \int_0^\infty I_{\lambda,(i)} \frac{1}{\pi} \rho_{\lambda,i}(\delta, \xi) d\lambda + \cos\beta_i \int_0^\infty E_{s,\lambda} \frac{1}{\pi} \rho_{\lambda,i}(\beta, \psi) d\lambda \qquad (4)$$

Introducing the dimensionless variables T_i', x_i', y_i', $q_{\text{net},i}'$, and t_i' into (2), together with the power law variation of conductivity and specific heat with temperature, one obtains

$$\frac{\partial^2 T_i'}{\partial x_i'^2} + \frac{\partial^2 T_i'}{\partial y_i'^2} + \frac{a_i}{T_i'}\left[\left(\frac{\partial T_i'}{\partial x_i'}\right)^2 + \left(\frac{\partial T_i'}{\partial y_i'}\right)^2\right] - \frac{\sigma L^2 T_0^{3-a_i}}{\bar{k}_i d_i} \frac{q_{\text{net},i}'}{(T_i')^{a_i}} + \frac{S_i L^2}{\bar{k}_i T_0^{1+a_i}} \frac{1}{(T_i')^{a_i}} = (T_i')^{b_i - a_i} \frac{\partial T_i'}{\partial t_i'} \qquad (5)$$

where

$$q_{\text{net},i}' = \int_{hs} I_i' \cos\theta_i\, d\omega_i - \sum_{j \neq i} \int_{A_j'} I_j' \times \frac{\cos\alpha_i \cos\theta_j}{(r_{ij}')^2} dA_j' - \int_{A_{(i)}'} I_{(i)}' \times \frac{\cos\delta_i \cos\theta_{(i)}}{[r_{i(i)}']^2} dA_{(i)}' - E_s' \cos\beta_i \qquad (6)$$

In (6), the dimensionless radiosities, such as I_i' (T_i', θ_i, ϕ_i), are given by

$$I_i' = \int_0^\infty I_{b,\lambda}'(T_i')\epsilon_{\lambda,i}\, d\lambda + \sum_{j \neq i} \int_{A_j'} \frac{\cos\alpha_i \cos\theta_j}{(r_{ij}')^2} dA_j' \int_0^\infty I_{\lambda,j}' \frac{1}{\pi} \times \rho_{\lambda,i}(\alpha, \gamma) d\lambda + \int_{A_{(i)}'} \frac{\cos\delta_i \cos\theta_{(i)}}{[r_{i(i)}']^2} dA_{(i)}' \int_0^\infty I_{\lambda,(i)}' \times \frac{1}{\pi} \rho_{\lambda,i}(\delta, \xi) d\lambda + \cos\beta_i \int_0^\infty E_{s,\lambda}' \frac{1}{\pi} \rho_{\lambda,i}(\beta, \psi) d\lambda \qquad (7)$$

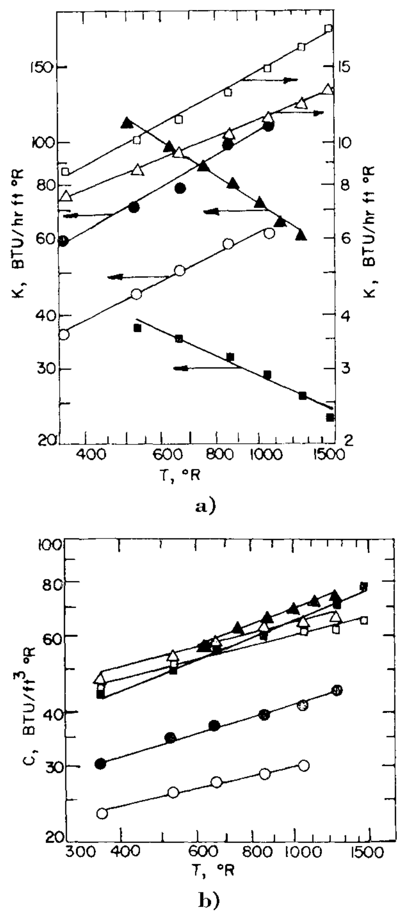

Fig. 2. Variation of thermal conductivity and heat capacity with temperature for several materials (see Table 1). △ = **301 SS,** ○ = **Mg,** ● = **Al,** □ = **monel,** ■ = **steel, and** ▲ = **Be.**

in which $I_{b,\lambda}'(T_i')$ is interpreted to mean

$$\frac{1}{\pi} \frac{C_1 \lambda^{-5}}{[\exp(C_2/\lambda T_0 T_i')] - 1} \frac{1}{\sigma T_0^4}$$

and $\epsilon_{\lambda,i}$ implies $\epsilon_{\lambda,i}(T_0 T_i', \theta_i, \phi_i)$, etc.

Equations (5–7) represent a general formulation, in dimensionless form, of the governing equations for the temperature distribution in an arbitrary surface A_i, which is exchanging radiant energy with $(n - 1)$ other surfaces. A similar group of equations could be written for a geometrically similar model similarly oriented with respect to the incident solar radiation. If complete similitude is to exist between the model and its prototype, these dimensionless equations must be identical. If the initial temperature field and boundary conditions are similarly prescribed, then by inspection one arrives at the following scaling criteria.

Steady-State Criteria

$$a_i^* = a_i \qquad (8a)$$

$$(L^*)^2 (T_0^*)^{3-a_i^*}/\bar{k}_i^* d_i^* = L^2 T_0^{3-a_i}/\bar{k}_i d_i \qquad (8b)$$

$$S_i^*(L^*)^2/\bar{k}_i^*(T_0^*)^{1+a_i^*} = S_i L^2/\bar{k}_i T_0^{1+a_i} \qquad (8c)$$

$$\int_0^\infty I_{b,\lambda}(T_i^*)\epsilon_{\lambda,i}^* d\lambda = \left(\frac{T_0^*}{T_0}\right)^4 \int_0^\infty I_{b,\lambda}(T_i)\epsilon_{\lambda,i} d\lambda \qquad (8d)$$

$$\int_0^\infty I_{\lambda,j}^* \rho_{\lambda,i}^*(\alpha, \gamma) d\lambda = \left(\frac{T_0^*}{T_0}\right)^4 \int_0^\infty I_{\lambda,j} \rho_{\lambda,i}(\alpha, \gamma) d\lambda \qquad (8e)$$

$$\int_0^\infty I_{\lambda,(i)}^* \rho_{\lambda,i}^*(\delta, \xi) d\lambda = \left(\frac{T_0^*}{T_0}\right)^4 \int_0^\infty I_{\lambda,(i)} \rho_{\lambda,i}(\delta, \xi) d\lambda \qquad (8f)$$

$$\int_0^\infty E_{s,\lambda}^* \rho_{\lambda,i}^*(\beta, \psi) d\lambda = \left(\frac{T_0^*}{T_0}\right)^4 \int_0^\infty E_{s,\lambda} \rho_{\lambda,i}(\beta, \psi) d\lambda \qquad (8g)$$

$$E_s^*/E_s = (T_0^*/T_0)^4 \qquad (8h)$$

If thermal contact resistance is of importance, an additional criterion arises. For joints between similar materials, it is given by

$$\bar{k}_i^*(T_0^*)^{a_i}/h_{J,i}^*L^* = \bar{k}_iT_0^{a_i}/h_{J,i}L \tag{8i}$$

which follows immediately from the definition of joint conductance, i.e., $[-k(\partial T/\partial x)]_{\text{joint}} = h_J\Delta T$, where ΔT is the temperature drop across the interface due to imperfect contact. It is not clear at the present time how (8*i*) should be modified for joints between dissimilar materials. A recent exposition of the physical nature of thermal contact resistance is given in Ref. 15.

If there is a prescribed heat flux over a portion of the prototype surface, one requires

$$q_{A,i}^*L^*/\bar{k}_i^*(T_0^*)^{1+a_i^*} = q_{A,i}L/\bar{k}_iT_0^{1+a_i} \tag{8j}$$

which insures similarity in the boundary condition.

When mutual irradiation among surfaces is not of significance, the second and third term on the right-hand sides of (3) and (4) may be set to zero. Since,

$$\int_{hs}\cos\theta_i d\omega_i \int_0^\infty I_{b,\lambda}(T_i)\epsilon_{\lambda,i}d\lambda = \epsilon_i\sigma T_i^4$$

and

$$\int_h \cos\theta_i d\omega_i \int_0^\infty E_{s,\lambda}\frac{1}{\pi}\rho_{\lambda,i}(\beta,\psi)d\lambda = \rho_{s,i}E_s$$

where ϵ_i is the total hemispherical emissivity of the surface A_i, and $\rho_{s,i}$ is its total hemispherical reflectivity with respect to solar radiation, one has under such condition

$$q_{\text{net},i} = \epsilon_i\sigma T_i^4 - (1-\rho_{s,i})E_s\cos\beta_i = \epsilon_i\sigma T_i^4 - \alpha_{s,i}E_s\cos\beta_i \tag{3a}$$

The criteria (8b–8h), with the exception of (8c), reduce to

$$\epsilon_i^*(L^*)^2T_0^{3-a_i^*}/\bar{k}_i^*d_i^* = \epsilon_iL^2T_0^{3-a_i}/\bar{k}_id_i \tag{8b$'$}$$

and

$$\alpha_{s,i}^*E_s^*/\epsilon_i^*(T_0^*)^4 = \alpha_{s,i}E_s/\epsilon_iT_0^4 \tag{8h$'$}$$

For constant conductivity, a_i vanishes and $\bar{k}_i$ becomes k_i. If one now multiplies (8b′) by (8h′) and uses the relation $L^*/d_i^* = L/d_i$, there is obtained

$$\alpha_{s,i}^*E_s^*L^*/k_i^*T_0^* = \alpha_{s,i}E_sL/k_iT_0 \tag{8h$''$}$$

which is criterion (7) given in Ref. 10. In view of the foregoing analysis, it is seen that (8h″) holds only under the condition stated. On the other hand, the similarity parameters listed in Table 1 of Ref. 11 appear to be in error.

Transient Criteria

In addition to the steady-state requirements, one needs the transient criteria,

$$b_i^* - a_i^* = b_i - a_i \tag{9a}$$

which reduces to $b_i^* = b_i$ when (8a) is satisfied, and

$$t_i'^* = t_i' \tag{9b}$$

with $t_i^*/t_i = \text{const}$, for all surfaces. We note that, in (8a–9b), $i, j = 1, 2, 3, \ldots, n$, but $i \neq j$.

An examination of the foregoing criteria reveals that complete similitude cannot, in general, be achieved. However, modeling may still be employed to yield useful information by demanding satisfaction of the important criteria but only approximate satisfaction of others. Factors to be considered are: 1) nature of the temperature field: two- or three-dimensional, steady or nonsteady, 2) relative importance of the temperature dependency of the bulk properties of materials (k and c) as compared to their surface properties (ϵ_λ and ρ_λ), and 3) number of different materials used in the spacecraft.

Two different techniques may be used for satisfying the modeling criteria. They will be referred to as "temperature preservation" and "material preservation." As the names suggest, "temperature preservation" means that temperatures are identical at homologous locations and times for the model and prototype, whereas "material preservation" implies that identical materials are used for corresponding parts of the model and prototype. These two techniques will be separately examined.

Temperature Preservation

In this case, $T_0^* = T_0$, and one attempts to satisfy the modeling criteria by using different materials for the model from those used for the prototype. Criterion (8a) remains as is, but (8b) becomes

$$\bar{k}_i^*/\bar{k}_i = (L^*/L)^2 d_i/d_i^* \tag{10a}$$

For strict geometric similarity, one would require $d_i^*/d_i = L^*/L$. However, since here we are concerned with spacecraft structures composed of thin sheets or shells, d^* can be reasonably arbitrary so long as the temperature field in the model remains two-dimensional. Some consideration may have to be given to the practical difficulties encountered in model fabrication.

We shall illustrate the procedure of approximately satisfying (8a) and (10a) by an example. Let us assume that a surface A_i is fabricated of AN-M-29 magnesium alloy and that its temperatures fall between 500° and 800°R. From Fig. 2, one sees that the average conductivity of this magnesium alloy is approximately 50 Btu/hr-ft-°R for the temperature range cited. If a model of $\frac{1}{5}$ scale is to be constructed ($L^*/L = \frac{1}{5}$), and if one chooses to use metal sheets of proportionate thickness, then $k_i^* \simeq k_i(L^*/L)$. Thus a material of conductivity in the neighborhood of 10 Btu/hr-ft-°R is appropriate. An important consideration is to select materials that exhibit similar temperature dependency. Referring to Fig. 2, one sees that Monel "K" approximately satisfies these requirements.§ We note: $a_i = 0.497$, $a_i^* = 0.555$; $\bar{k}_i = 1.99$, $\bar{k}_i^* = 0.315$; hence $d_i^*/d_i = (L^*/L)^2(\bar{k}_i/\bar{k}_i^*) = 0.252$. When the prototype consists of surfaces made of several different materials, advantage can be taken of the relative freedom that one has in choosing the thicknesses. A major difficulty lies in the satisfaction of the condition $a_i^* = a_i$. The artificial means of modifying conductivity of a given material by "slitting" as suggested by Katzoff[8] may provide for a solution to the problem, though care must be exercised to avoid altering the surface properties by any significant amount.

There appears to be no serious difficulty imposed by criterion (8c). It is

$$S_i^*/S_i = d_i/d_i^* \tag{10b}$$

Criteria (8d–8h) will be satisfied if the monochromatic directional emissivities and reflectivity functions at homologous locations of the model and prototype are identical, and if the solar radiation is identically simulated. In principle, the desired surface properties may be obtained by appropriate coating, but not without experiencing possible difficulties. Katzoff[8] pointed out that " . . . coating thicknesses cannot normally be scaled without changing the optical properties, therefore, some corresponding allowances for the coating mass, conductance, and heat capacity may have to be made when a fairly heavy coating is applied to relatively thin sheet material." Means of producing radiation that approximates the solar spectrum has been described in the literature.[2–4]

§ The search for suitable material has not been exhaustive; a better choice is undoubtedly possible. Here, a_i^* differs from a_i by nearly 12%, and thus may not be acceptable in accurate model work.

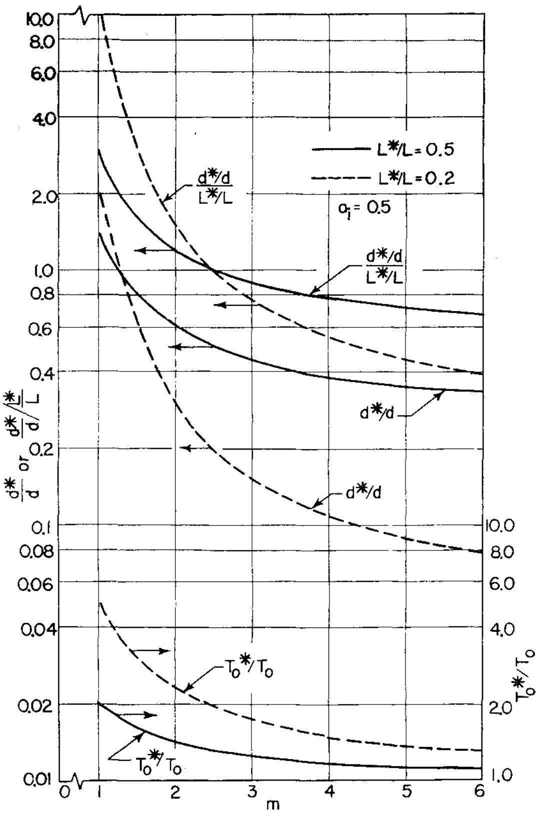

Fig. 3 Variation of temperature, thickness, and thickness distortion factors with m.

Criteria (8*i*) and (8*j*) become, respectively,

$$h_{J,i}^*/h_{J,i} = 1 \tag{10c}$$

$$q_{A,i}^*/q_{A,i} = 1 \tag{10d}$$

It is important that the right-hand side of (10c) or (10d) is not written as (L^*/L) (d_i/d_i^*) when 'distorted' model thickness is used. There will be some local error in the temperature field at the vicinity of the joint where the heat flow can no longer be two-dimensional.

For transient problems, two additional requirements have to be met. Criterion (9a) remains as is, and (9b) becomes

$$t_i^*/t_i = (d_i^*/d_i)(\bar{c}_i^*/\bar{c}_i) \tag{10e}$$

Equation (9a) can only be satisfied by a judicious selection of the material. Since the thickness ratio d_i^*/d_i has already been fixed, the time scaling factor is thus dictated by (10e). Inasmuch as t_i^*/t_i must be the same for all i's, this constitutes the major handicap when more than one material is involved in the prototype, as is usually the case. However, if one uses the same material and the technique of "slitting" to obtain the desired thermal conductivity, as described by Katzoff, it appears reasonable to assume that the heat capacity will only be slightly affected. Furthermore, such an effect, if it arises, can be compensated for by an appropriate selection of the thickness ratio, because the conductivity ratio is now presumably under control of the designer, and thus the satisfaction of (10a) can be achieved without taking advantage of the freedom in the choice of d_i^*/d_i. More work, both theoretical and experimental, needs to be done to explore the potential of such possibilities.

Material Preservation

In this case, the corresponding members of the model and of the prototype are fabricated from identical materials. The temperatures at the homologous locations and times of the model and of the prototype differ by a constant scaling factor. Criterion (8a) is automatically satisfied, and (8b) becomes

$$T_0^*/T_0 = [(d_i^*/d_i)(L/L^*)^2]^{1/(3-a_i)} \tag{11a}$$

If $a_i = 0$, and $d_i^*/d_i = L^*/L$, one obtains $T_0^*/T_0 = (L/L^*)^{1/3}$, a known result.[8–11] For two-dimensional temperature fields, the thickness ratio is, to some extent, arbitrary. This provides flexibility in the selection of the temperature scaling factor. For convenience, let us consider

$$T_0^*/T_0 = (L/L^*)^{1/m} \tag{11b}$$

where m is a real, positive number. Substituting (11b) into (11a) gives,

$$d_i^*/d_i = (L^*/L)^{(2m-3+a_i)/m} \tag{11c}$$

Strict geometric similarity occurs when $m = 3 - a_i$. Figure 3 shows the variation of T_0^*/T_0 and d^*/d with m for $\frac{1}{2}$- and $\frac{1}{5}$-scale models. Included is a plot for the ratio $(d^*/d)/(L^*/L)$ which is a measure of model thickness distortion. For strictly geometrically similar models, this ratio is obviously unity. It is seen from the figure that, as m increases, both the temperature and thickness scaling factors decrease for a given geometric scaling factor. In general, when using the material preservation technique, the model criteria are better satisfied for small values of T_0^*/T_0, i.e., as the latter is closer to unity. Hence, it appears desirable to choose m as large as possible, consistent with the minimum thickness that is feasible in model construction.

Criterion (8c) would again cause no serious difficulty. It is

$$S_i^*/S_i = (L/L^*)^{(2m+1+a_i)/m} \tag{11d}$$

Since

$$\sigma T^4 = \pi \int_0^\infty I_{b,\lambda}(T) d\lambda$$

criteria (8d–8f) would be satisfied if the monochromatic directional emissivity and reflectivity functions are independent of temperature and wavelength with respect to radiation originating from the surfaces themselves. This is necessary since, in the present technique, the temperatures at corresponding locations of the model and of the prototype are not the same. Let us now examine whether these requirements can realistically be met. It is known that radiation emitted from surfaces at temperatures of 1000°R or less is, for all practical purposes, limited to the region where $\lambda > 3\mu$. A survey of literature[16, 17] reveals that, for many engineering materials, the monochromatic emissivities and reflectivities are weak functions of wavelengths for $\lambda > 3\mu$. They become strongly dependent on λ only for shorter wavelengths. Reference 17 also reports that, within reasonable temperature limits, the surface properties of many of these same materials are also weak functions of temperature. It is pertinent that the directional variation of these properties does not constitute a problem since geometrically similar model surfaces are employed.

Criteria (8g) and (8h) concern solar radiation. Over 99% of solar radiation is confined to the region where the wavelength is less than 3μ.[18] In this region, as noted previously, the reflectivity function is strongly dependent on λ. However, (8g) may still be satisfied provided that 1) the monochromatic reflectivity function is independent of the temperature of the surfaces and 2) the simulated solar radiation has a spectral distribution identical to that of the sun but with its intensity scaled according to

$$E_{s,\lambda}^*/E_{s,\lambda} = (T_0^*/T_0)^4 \tag{11e}$$

It is apparent from the foregoing considerations that the simultaneous satisfaction of criteria (8d–8g), with due consideration of the dependence of ρ_λ on λ for $\lambda < 3\mu$, requires that a limit be placed on the maximum temperature of the

Table 2 Variation of time scale factor (t_i^*/t_i) due to unequal values of ($a - b$): two-dimensional temperature field[a]

	$L^*/L = 0.5$					$L^*/L = 0.2$				
$a_i - b_i$	$m = 2$	$m = 3$	$m = 4$	$m = 5$	$m = 6$	$m = 2$	$m = 3$	$m = 4$	$m = 5$	$m = 6$
0.174	0.235	0.240	0.243	0.244	0.246	0.0348	0.0362	0.0371	0.0379	0.0382
0.271	0.228	0.235	0.238	0.241	0.242	0.0322	0.0346	0.0357	0.0368	0.0370
0.278	0.226	0.234	0.238	0.241	0.242	0.0340	0.0343	0.0357	0.0367	0.0370
0.345	0.220	0.231	0.236	0.238	0.240	0.0295	0.0332	0.0349	0.0357	0.0362
−0.885	0.340	0.307	0.291	0.282	0.276	0.0820	0.0640	0.0570	0.0530	0.0505
−1.073	0.362	0.320	0.301	0.290	0.283	0.0945	0.0710	0.0615	0.0565	0.0530

[a] Perfect modeling requires a constant t_i^*/t_i for all surfaces.

surfaces. For a $\frac{1}{5}$-scale model, one may readily show that $T_0^*/T_0 = 1.495$, if $m = 4$. The corresponding intensity ratio $E_{s,\lambda}^*/E_{s,\lambda}$ is 5. On the other hand, if one selects m to be 6, the required intensity ratio reduces to 2.93, thus offering a possible advantage in model simulation. It is recognized that, with the present technology, this is still regarded as a handicap. Criterion (8h) is automatically satisfied when condition (11c) is fulfilled. Criteria (8i) and (8j) now assume the following form:

$$h_{J,i}^*/h_{J,i} = (L/L^*)^{3/(3-a_i)} \tag{11f}$$

$$q_{A,i}^*/q_{A,i} = (L/L^*)^{4/(3-a_i)} \tag{11g}$$

When values of m other than $(3-a_i)$ are used, some local disturbance in the temperature field will occur.

For transient problems, criterion (9a) is automatically satisfied in the "material preservation" technique, whereas (9b) becomes

$$t_i^*/t_i = (L^*/L)^{(2m+a_i-b_i)/m} \tag{11h}$$

Again, since t_i^*/t_i has to be identical for all i's, one immediately requires that $(a_i - b_i)$ be the same for all surfaces. In general, this condition cannot be met. In Table 1, the values of $(a_i - b_i)$ are listed for the six materials referred to in Fig. 2. To ascertain the influence of not having identical values of $(a - b)$ on the feasibility of transient modeling, Table 2 is prepared. There is shown the variation of the time scaling factor t_i^*/t_i among the six materials for $L^*/L =$ 0.2 and 0.5, and for m ranging from 2 to 6. If one excludes SAE 1010 steel and beryllium, and if one considers a $\frac{1}{2}$-scale model, the maximum deviation from the mean amounts to 1.7% if $m = 4$. The corresponding maximum deviation for the $\frac{1}{5}$-scale model is 3.3%. Here, again, the advantage of choosing large values of m is obvious.

Generalization to Three-Dimensional Temperature Fields

The similarity criteria may be deduced in precisely the same manner as described previously. The governing differential equation for the temperature field is simpler and is given by

$$\operatorname{div}(k_i \operatorname{grad} T_i) + S_i = c_i \partial T_i/\partial t \tag{12}$$

The radiative transfer enters only through the boundary condition. After carrying out the analysis, one finds that, with the exception of (8b), the required criteria are identical to those for the two-dimensional case, namely (8a–8h, 9a and 9b). Criterion (8b) becomes

$$L^*(T_0^*)^{3-a_i^*}/\bar{k}_i^* = LT_0^{3-a_i}/\bar{k}_i \tag{13}$$

Clearly, in this case, all of the flexibility resulting from the freedom in the selection of model thickness in two-dimensional problems is lost. For brevity's sake, we merely present the results as follows.

Temperature Preservation

Criteria (10a, 10b, and 10c) should be replaced, respectively, by

$$\bar{k}_i^*/\bar{k}_i = L^*/L \tag{14a}$$

$$S_i^*/S_i = L/L^* \tag{14b}$$

$$t_i^*/t_i = (L^*/L)(\bar{c}_i^*/\bar{c}_i) \tag{14c}$$

Criteria (10c) and (10d) remain unaltered. The satisfaction of (14a) and (14c), together with the requirements $a_i^* = a_i$ and $b_i^* = b_i$, becomes extremely difficult when a number of different materials is involved in the prototype. A possibility would be to develop means to artificially control the thermal conductivity without adversely affecting the heat capacity (e.g., the 'slitting' technique for two-dimensional problems). At the present time, it is not known how this could be achieved in practice.

Material Preservation

Criterion (11a) becomes

$$T_0^*/T_0 = (L/L^*)^{1/(3-a_i)} \tag{15a}$$

which must be a constant for all members of the model. This requires a_i to be independent of i (a condition that cannot be satisfied in general). Table 3 illustrates the variation in the temperature scaling factor for the six materials. If only stainless steel, magnesium, aluminum and Monel "K" (first four) are involved in the modeling, the maximum deviation in the ratio T_0^*/T_0 from its mean is 1.1% for the $\frac{1}{2}$-scale model and 2.9% for the $\frac{1}{5}$-scale model.

Criteria (11b) and (11c) obviously do not apply, (11d) should be replaced by

$$S_i^*/S_i = (L/L^*)^{(7-a_i)/(3-a_i)} \tag{15b}$$

while criteria (11e–11g) remain unaltered. The transient criterion (11h) now becomes

$$t_i^*/t_i = (L^*/L)^{2+(a_i-b_i)/(3-a_i)} \tag{15c}$$

which implies that $(a_i - b_i)/(3 - a_i)$ has to be independent of i since all the members must have identical time scaling factor. Table 4 shows the variation of the time scale factor among the six materials for the $\frac{1}{2}$- scale and $\frac{1}{5}$-scale models. Again, leaving out the SAE 1010 steel and beryllium (last two), one finds that the maximum deviation in the ratio of t^*/t from its mean is 3% for the $\frac{1}{2}$-scale model and 6.8% for

Table 3 Variation of temperature scale factor among the six materials (three-dimensional case)

	T_0^*/T_0	
a	$L^*/L = 0.5$	$L^*/L = 0.2$
0.395	1.305	1.855
0.497	1.319	1.900
0.580	1.332	1.945
0.555	1.327	1.930
−0.485	1.220	1.587
−0.656	1.209	1.555

Table 4 Variation of time scale factor among the six materials (three-dimensional case)

a	t_i^*/t_i	
	$L^*/L = 0.5$	$L^*/L = 0.2$
0.395	0.239	0.0360
0.497	0.232	0.0338
0.580	0.231	0.0333
0.555	0.227	0.0319
−0.485	0.298	0.0602
−0.656	0.307	0.0641

the $\frac{1}{5}$-scale model. As previously noted, in the two-dimensional case, this error could be reduced by selecting large values of m. No such freedom exists in the three-dimensional case.

As a final remark, we reiterate that, with the material preservation technique, the model operates at temperatures higher than those of the prototype. The smaller the scaled model, the higher its temperatures will be. One thus encounters all the adverse effects inherently associated with such operation, namely, dimensional instability and warpage, changes in surface and bulk properties, deterioration of surface paints, variations in joint conductances, etc. The requirement imposed by (11e) alone seems already very severe and, finally, the problem of obtaining accurate temperature measurements in scaled down models with large temperature gradients could be formidable.

References

[1] Mark, H., "Operation of a solar space environment simulator," *Proceedings of the Institute of Environmental Sciences* (Institute of Environmental Sciences, Illinois, April 1961), pp. 521–531.

[2] Uguccini, O. W. and Pollack, J. L., "A carbon-arc solar simulator," American Society of Mechanical Engineers Paper 62-WA-241 (1962).

[3] Levene, M. L. and Lauxen, C., "Continuous carbon-arc for solar simulation," American Society of Mechanical Engineers Paper 62-WA-331 (1962).

[4] Freeman, R. S., "Continuously operating carbon-arc lamp for solar simulation," American Society of Mechanical Engineers Paper 62-WA-208 (1962).

[5] Katz, A. J., "Thermal testing," Space/Aeronaut. **38,** 30–34 (1962).

[6] Clark, L. G. and Laband, K. A., "Orbital station temperature control," Astronautics **7,** 40–43 (1962).

[7] Langhaar, H. L., *Dimensional Analysis and Theory of Models* (John Wiley and Sons, Inc., New York, 1951), Chap. 5, p. 64.

[8] Katzoff, S., "Similitude in thermal models of spacecraft," NASA TN D-1631 (April 1963).

[9] Clark, L. G., "Temperature balance of manned space stations," NASA TN D-1504, Part 3 (August 1962).

[10] Vickers, J. M. F., "A study of thermal scale modeling techniques," *ASD-AIA Symposium on Aeroelastic and Dynamic Modeling Technology,* Office of Technical Service, U.S. Dept. of Commerce, Doc. RTD-TDR-63-4197, Part I, pp. 97–126 (September 1963).

[11] Wainwright, J. B., Kelley, L. R., and Keesee, T. H., "Modeling criteria and testing techniques for the simulation of space environments," Fourth Annual Symposium on Space Environment Simulation, Los Angeles, Calif., pp. 1–14 (May 1963).

[12] Goldsmith, A., Waterman, T. E., and Hirschorn, H. J., *Handbook of Thermophysical Properties of Solid Materials* (The MacMillan Co., New York, 1961), Vols. I, II, and III.

[13] Lucks, G. F. and Deem, H. W., "Thermal properties of thirteen metals," American Society for Testing Materials Special Tech. Publ. 227 (1958).

[14] *Metallic Elements and Their Alloys* (Thermophysical Properties Research Center, Purdue Research Foundation, Lafayette, Ind., 1960).

[15] Clausing, A. M. and Chao, B. T., "Thermal contact resistance in a vacuum environment," American Society of Mechanical Engineers Paper 64-HT-16; also J. Heat Transfer (to be published).

[16] Gier, J. T., Dunkle, R. V., and Bevans, J. T., "Measurement of absolute spectral reflectivity from 1.0 to 15 microns," J. Opt. Soc. Am. **14,** 558–562 (1954).

[17] Gubareff, G. G., Janssen, J. E., and Torborg, R. H., *Thermal Radiation Properties Survey* (Minneapolis-Honeywell Regulator Co., Minneapolis, Minn., 1960).

[18] Johnson, F. S., "The solar constant," J. Meteorol. **11,** 431–439 (1954).